# Physics of single molecule fluctuations in surface enhanced Raman spectroscopy active liquids

R. C. Maher
*The Blackett Laboratory, Imperial College London Prince Consort Road, London SW7 2BW, United Kingdom*

M. Dalley
*The McDiarmid Institute for Advanced Materials and Nanotechnology, School of Chemical and Physical Sciences, Victoria University of Wellington, P.O. Box 600 Wellington, New Zealand*

E. C. Le Ru
*The McDiarmid Institute for Advanced Materials and Nanotechnology, School of Chemical and Physical Sciences, Victoria University of Wellington, P.O. Box 600 Wellington, New Zealand*

L. F. Cohen
*The Blackett Laboratory, Imperial College London Prince Consort Road, London SW7 2BW, United Kingdom*

P. G. Etchegoin[a)]
*The McDiarmid Institute for Advanced Materials and Nanotechnology, School of Chemical and Physical Sciences, Victoria University of Wellington, P.O. Box 600 Wellington, New Zealand*

H. Hartigan, R. J. C. Brown, and M. J. T. Milton
*National Physical Laboratory, Queen's Road, TW11 OLW Teddington, Middlesex, United Kingdom*

(Received 21 July 2004; accepted 16 August 2004)

Surface enhanced Raman spectroscopy (SERS) of dyes in solution allows the study of the differences between ensemble averaged spectroscopic signals and single molecular events. We address several outstanding issues in single molecule detection via SERS; in particular, evidence for single molecule vibrational pumping and/or single molecule laser heating, the statistics of hotspots in the liquid, and anti-Stokes/Stokes anomalies. We demonstrate that anti-Stokes/Stokes ratios are a very unreliable measure of temperature, because the two processes are affected differently by the underlying frequency-dependent plasmon resonances. Subtle hints of vibrational pumping and/or heating in single molecules can only obtained via careful cross correlations between the parameters (frequency position, width, and intensity) of the Stokes signals for different excitation lasers. We introduce the use of single-peak parameter cross correlations for the study of these phenomena. © *2004 American Institute of Physics.* [DOI: 10.1063/1.1804178]

## I. INTRODUCTION AND OVERVIEW

Surface enhanced Raman scattering (SERS)[1,2] is a technique capable of detecting single molecules in a wide variety of cases. From the analytical chemistry standpoint, SERS is, in principle, a technique with the ultimate resolution for the tracing of certain types of molecules (mainly dyes). But attempts in the past to transform the single-molecule capabilities of the technique into a reliable analytical tool at ultradiluted concentrations have failed in general. One of the main possible applications of SERS is in the field of cell and molecular biology. A nanomol is a typical concentration of interest in biology; it corresponds approximately to the dilution of the chemical content of a pill in the size of a human body. Nanomolar concentrations of dyes can be easily detected with SERS, but the same holds for fluorescence spectroscopy (FS); which has a longstanding history of success and it is in many cases preferred due to the simpler instrumentation and interpretation of the spectra. SERS competes with FS at concentrations beyond the nanomolar range. In the pico to femto-molar ranges, understanding issues of single-molecular detection become mandatory. SERS has several potential advantages in that range, the most important of which is the chemical specificity, which helps to overcome background problems affecting FS in transient signals. But SERS experiments have to overcome still issues of reproducibility in the quantification of signals before it can be used routinely as an anlytical tool in this ultradiluted concentration range. There are several reasons for this failure; the most salient of them is the fact that single-molecule detection (SMD) with SERS is achieved under the condition known as *amplification* via *hotspots*. Hotspots are believed to be highly localized optically active surface plasmon resonance interactions, appearing in metallic nanostructures with complex topologies. They are believed to provide small (even subwavelength[3,4]) regions where the average enhancement factors of the electromagnetic field can be very large (by several orders of magnitude). Different claims in the literature put the maximum enhancement factors in different

[a)]Electronic mail: Pablo.Etchegoin@vuw.ac.nz

 

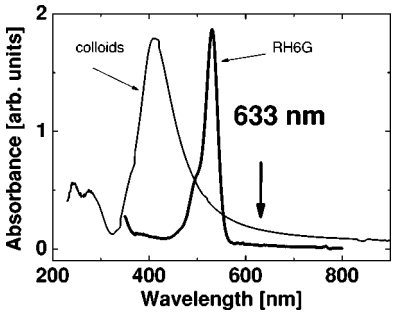


FIG. 1. Uv-visible absorbance spectrum of citrate reduced Ag colloids in a 10 mM KCl solution. The spectrum is dominated by the single-colloid surface plasmon resonance at ~410 nm. The position of the laser (HeNe) with respect to the main absorption peak is also shown in the figure. The HeNe-laser profits from sporadic transient plasmon resonances, which are red-shifted with respect to the main absorption peak (Ref. 4), but do not contribute much to the absorption spectrum because they only happen dynamically and they are sparsely distributed. The absorption of RH6G is also shown for completeness. The 633 nm HeNe laser is below the main absorption of RH6G in the transparency region. The intensities of both absorptions are in arbitrary units and are not directly comparable.

ranges, from $10^8$ to $10^{15}$. Regardless of the discrepancies in the literature, there is widespread consensus that SMD is achievable in a wide variety of situations.[5–7]

With the aim of contributing to the understanding of what it is actually measured, and how it should be interpreted, this paper concentrates on two specific aspects of the SERS-SMD problem in solutions: (i) The existence of hidden inhomogeneous plasmon resonances affecting the intensity of the peaks and anti-Stokes/Stokes ratios (aS/S); and (ii) Evidence for laser-heating events and/or vibrational pumping. These two topics have been the subject of a still-ongoing discussion and discrepancy in the literature.

## II. EXPERIMENTAL DETAILS

Ag colloids for SERS were prepared by reduction of $AgNO_3$ using the standard technique introduced by Lee and Meisel.[8] Silver nitrate is reduced by sodium citrate (all chemicals purchased from Sigma), resulting in a brown-yellow colloidal suspension which is stable at room temperature for a number of weeks (and for several months at 4–5 °C). The absorption spectra of the suspensions show a characteristic single particle surface-plasmon peak at ~400 nm, shown in Fig. 1. Independent measurements of the particles using an atomic force microscope showed colloidal particles with diameters in the range ~60–65 nm.[9] We estimate the colloid concentration of the neat solution to be $\sim 10^{11}$ colloids/cm$^3$. We study SERS events in this colloidal liquid. The colloids are activated with a 20 mM KCl solution in a 50%–50% mixture with the colloids, immediately prior to the experiment (producing an effective 10 mM KCl concentration in the sample). The final concentration of the analyte (rhodamine 6G: RH6G) in the sample is either 10 nM or 1 $\mu$M depending on the experiment. Our choice of dye to show the effects we want to demonstrate in this paper is based on the overwhelming amount of work done on SERS of RH6G in the past. Our results on peak correlations, reported later, should be easily reproduced without the need for new dyes or further chemical aspects.

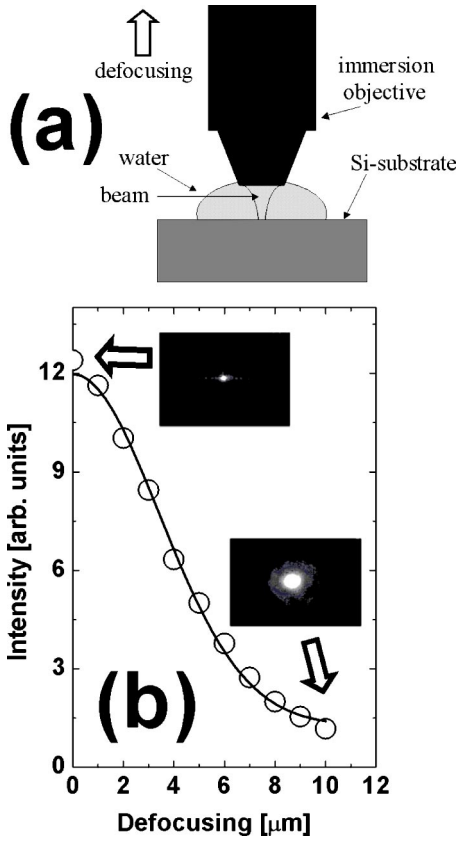


FIG. 2. Confocality test of the scattering volume. (a) The objective (immersed in water) is focused onto a Si wafer and the intensity of the 520 cm$^{-1}$ Raman active phonon is monitored as a function of the defocusing distance. In (b) we show the intensity profile and the two beam shapes at zero and maximum (10 $\mu$m) defocusing. The FWHM of this profile (~8 $\mu$m) defines the scattering length in the axial direction. The beam diameter ($d \sim 650$ nm) is determined with a similar test doing a line scan on a cleaved Si edge. The scattering volume $V_S$ is measured to be $\sim 2.65 \times 10^{-12}$ cm$^3$.

An important parameter of the experiment, requiring careful consideration, is the scattering volume of the immersion microscope. We use a Jobin-Yvon LabRam system coupled to an Olympus BX41 confocal microscope, equipped with an achromatic ×100 immersion objective index matched to water. The confocal pinhole of the instrument can be used to define different scattering volumes in the experiment. We used a 200 $\mu$m pinhole throughout and define the scattering volume $V_S$ by a confocal test on an immersed Si wafer. This is explicitly shown on Fig. 2. In the axial direction, the microscope detects events over a distance of $z \sim 8\ \mu$m; defined as the full width at half maximum (FWHM) of the intensity vs defocusing-distance profile in Fig. 2. This distance is adequate for the frequency of events we observe and within factory specifications for the 200 $\mu$m pinhole. In the radial direction, we perform edge beam profiling using the cleaved [110] edge of a Si wafer with a ×10 objective, and then rescale the diameter by a factor of 10. Direct edge-beam profiling with the ×100 is not possible due to diffraction at the edge and limitations in the stepper motor stage which has a resolution of 0.5 $\mu$m. We estimate the beam diameter to be $d \sim 650$ nm for the HeNe laser ($d \sim \lambda$). Our scattering volume turns out then to be

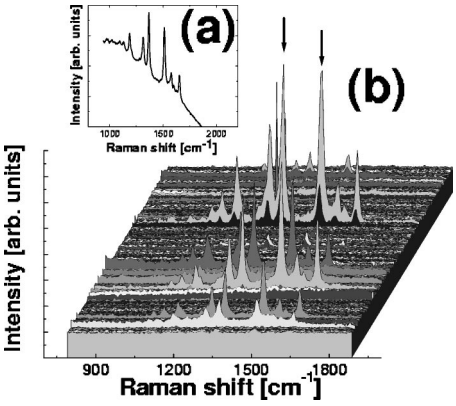


FIG. 3. Distinctive features of single-molecule spectra in SERS are (i) relative fluctuations of Raman active peaks, and (ii) fluorescence quenching. In (a) we show a spectrum taken for a concentrated 100 mM RH6G solution in water. The difference in background fluorescence is obvious from the data in (b) which is a time scan over 25 sec with 250 spectra. The Raman fluctuations in (b) are monitored in a 10 nM RH6G SERS active solution. The integration time for this scan was 0.1 sec with the CCD centered at 1360 cm$^{-1}$ on the Stokes side of the HeNe laser (2 mW). Note the presence of isolated single-molecule events separated by regions with zero intensity. The relative fluctuations of the two peaks labeled with arrows are shown in more detail in Fig. 4.

$V_S = \pi z d^2/4 \sim 2.6 \times 10^{-12}$ cm$^3$ under these conditions.

A 10 nM dilution of RH6G (molecular weights is 479) has $\rho_N \sim 6.02 \times 10^{12}$ molecules/cm$^3$; i.e., the microscope has an average of $N = \rho_N V_S \sim 15$ molecules at all times in the scattering volume. A similar analysis can be made for the 514 nm $Ar^+$-laser line, with $N \sim 10$, being slightly smaller. These numbers are transformed into $\sim 1500$ and $\sim 1000$ molecules for a 1 $\mu$M solution. Another important parameter of the experiment is the diffusion (or transit) time $\tau_D$ of the dyes across $V_S$. From simple diffusion theory $\tau_D \sim V_S^{2/3}/(2D)$, where $D$ is the diffusion coefficient. Taking $D \sim 10^{-5}$ cm$^2$/sec, typical of many dyes in water,[10] we obtain a characteristic transit time of $\tau_D \sim 1$ msec. The integration time $\tau$ for the $N_2$-cooled charge coupled device (CCD)-detector of the spectrometer is always between 0.1 and 1 sec, depending on the sample. $\tau = 0.1$ sec is the minimum we can use in a time dependent measurement, limited by the readout time of the CCD. If the system were detecting a signal from every dye coming inside $V_S$, over a period of $\sim 0.5$ sec the instrument should register the signal of $\sim 500-1000$ molecules. We used varying laser power on the samples from 2 to 20 mW at either 633 or 514 nm; we specify the conditions in each case where appropriate.

Dynamic light scattering (DLS) was used as an aid to estimate particle and cluster sizes. DLS experiments have been performed on a Malvern particle size analyzer using a digital autocorrelator and a 50 mW solid-state green ($\lambda = 532$ nm) diode laser.

## III. RESULTS AND DISCUSSION

### A. Hotspot statistics

Figure 3 shows a typical monitoring of the signal with the objective immersed in a solution with 10 nM RH6G in the SERS active colloids. Each spectrum is taken every 0.1 sec with the CCD centered at a Raman shift of 1360 cm$^{-1}$ on the Stokes side of the HeNe laser (2 mW). The careful characterization of the scattering volume, together with the number of molecules contained in it and the fact that $\tau \gg \tau_D$, allows us to conclude that hotspots are effectively rare events in the liquid and we are obviously not seeing all the molecules that transit the scattering volume during the integration time. If we were observing every single molecule entering $V_S$ we would have to observe the integrated signal of $\sim 50-100$ molecules. This is not, however, what it is observed experimentally. The signal completely disappears in between spectra that show very large and clear Raman signatures of RH6G. It has been speculated in the past that we could *count* a small number of single-molecule events in a colloidal fluid[6] by either flushing a microdroplet of liquid through a laser or *mapping* a small drop contained in a microfluidic channel. These methods, however, rely very strongly on the statistics and nature of the hotspots created in a fluid. The careful characterization of $V_S$ performed here reveals that, in standard situations hotspots are rare. The obvious reason for this is the sparsity of small clusters in the liquid, produced by the presence of KCl. The colloids by themselves without KCl show relatively small SERS signals. A simple calculation for our samples show that in the original solution we have an average of 0.25 colloids in the scattering volume. This means that, in the best possible situation, we might see two colloids coming close to each other in the scattering volume in the neat solution. This, however, seems to be very ineffective to produce hotspots with large enhancements because there is a minimum screening distance below which the colloids cannot approach each other. The addition of KCl nucleates small clusters of colloids up to a certain size, which remain floating in the liquid by buoyancy. Preliminary data taken with DLS of the neat and KCl-mixed solutions indicate this transition in size from single colloids to small clusters. The results here show the importance of understanding the *convoluted problem of analyte concentration with the statistic of hotspots*. A SERS signal cannot be observed if either one or the other is missing. The infrequent occurrence of hot-spots can be compensated to a large degree by averaging methods and integration times for quantification purposes, but this is precisely where a detailed understanding of the statistics of hotspots is required.

By the same token, we can infer from the data in Fig. 3 that these are truly single molecule events; the sparsity of the data makes two or more molecules events extremely rare. We are in the limit in which a histogram of intensities of a single peak for a long period of time reveals no substructure of two or three molecules scattering events, as demonstrated previously.[6] One important question at this stage is in which aspects single molecule spectra from RH6G differ from an ensemble average. This allows us to turn the attention of the analysis to the details of transient single-molecule scattering events and, in particular, anomalies and evidence for single molecule laser heating.

### B. Single versus ensemble averaged signals

The first obvious difference between single and ensemble averaged data is fluorescence quenching; a phenom-

enon reported in many previous SERS experiments and coming,[11] presumably, from rapid quenching of excitations in the molecule into the metal. We shall argue later that these relaxation mechanism might be responsible for the relatively small effect of laser heating. The inset of Fig. 3 shows the spectrum of RH6G taken with the same laser and objective in a 100 mM solution in water (no colloids) where the relative intensity of fluorescence and Raman signals can be seen.

In addition, there are more subtle differences also in the spectrum of a single dye. The most interesting one is the observation of changes in the relative intensities of various peaks. It is well known for RH6G that the most intense Raman modes come from totally symmetric $A_g$ modes of stretching in-plane C-C vibrations of the main backbone.[12,13–14] The structure of RH6G can be thought of as a combination of a main backbone with a side moiety resembling ethyl benzoate. The intense Raman modes come from the backbone and are all represented by a highly uniaxial Raman tensor.[12,13] Vibrations with a highly uniaxial tensor show, in large ensemble averages, a depolarization ratio $\rho \equiv I_\perp / I_\parallel = 1/3$, where $I_\perp$ and $I_\parallel$ are the perpendicular and parallel polarized Raman intensities from a homogeneous liquid.[15] Effectively, ratios of parallel ($I_\parallel$) and perpendicularly ($I_\perp$) polarized Raman spectra taken in a concentrated solution of RH6G in water (100 mM) with the HeNe laser reveal that the depolarization ratio rule of $I_\perp / I_\parallel \sim 1/3$ is fulfilled to a very good approximation for all the intense modes.

In the single molecule SERS condition, however, intensities of different modes are seen to vary considerably among themselves. Figure 4 shows selected transient single-molecule spectra taken in the liquid where the relative intensities of different peaks are compared. The relative intensities of the two modes highlighted in Fig. 3(b) are explicitly compared in three different selected spectra in Figs. 4(a), 4(b), and 4(c). Even larger fluctuations in relative intensities are seen for modes separated by larger energy differences, as exemplified in Fig. 4(d), where the relative intensity of the $\sim 610\ \mathrm{cm}^{-1}$ mode is compared to the intensity of the higher frequency modes at 1360 and $1510\ \mathrm{cm}^{-1}$. If different vibrations had different Raman tensors, and if the signal comes from only one molecule, one could argue that the relative intensities of the modes correspond to the specific orientation of the molecule with respect to the laser beam at the moment where the scattering event occurred. The fact that the symmetry of the modes is the same, precludes an explanation of this effect in terms of purely orientational effects. We shall show later that the most likely cause of these fluctuations is, precisely, the different couplings of the modes to local plasmon resonances, which is the same effect producing anomalous anti-Stokes/Stokes ratios.

The main conclusion we would like to carry to the following section is the experimental fact that single molecule events show large relative fluctuations of the most intense Raman peaks, an effect which cannot be easily ascribed to orientational effects and reflects the different couplings of different frequencies with the local plasmon resonance environment. In our opinion, these are the *hidden* resonances postulated by Moskovits and co-workers,[16] we shall give further justification of this statement in the theoretical section.

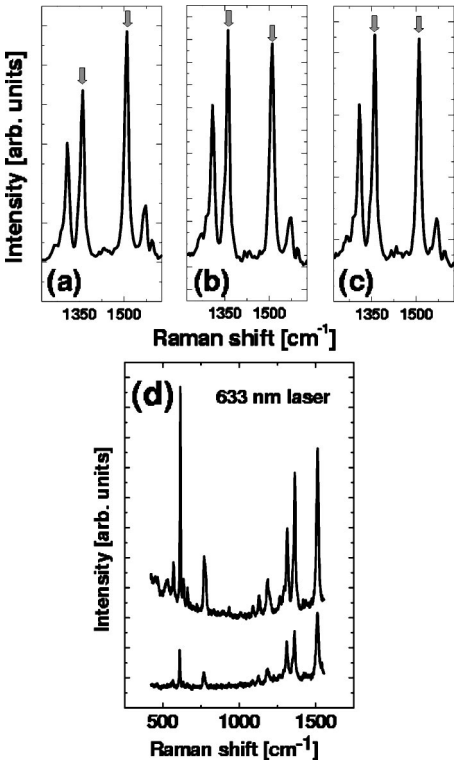


FIG. 4. All spectra in this figure correspond to different transient single-molecule SERS events in the experimental conditions of Fig. 3(b). In (a), (b), and (c) we show three examples of relative fluctuations between the 1360 and $1510\ \mathrm{cm}^{-1}$. Three different situations of larger, similar, and smaller relative intensities of one with respect to the other can be observed. Larger fluctuations in relative intensities can be observed for peaks further away in energy. An example is shown in (d) between the $610\ \mathrm{cm}^{-1}$ mode (of $A_g$ symmetry like the others) and the group of peaks around $1400\ \mathrm{cm}^{-1}$. Changes in relative intensities up to factors of 4 and 5 can be easily observed as a function of time. Different underlying resonances at different energies boost the different Raman peaks to different extents, producing changes in relative intensities. See the text for further details.

### C. Single-molecule Stokes/anti-Stokes scattering, laser heating, and vibrational pumping

Having established in the preceding section that large relative fluctuations can occur in Raman active modes at different energies for SMD, we now concentrate on how the different amplification of the modes affects the conclusion regarding single molecule laser heating or vibrational pumping. We propose essentially a different way to look at evidence for these effects based on correlations among peak parameters in single-molecular events.

A few years ago, Kneipp and co-workers[17] suggested the possibility of vibrational population pumping produced by the massive enhancements typical of off-resonance SERS; they suggested the possibility of observing scattering from the populated levels. The argument runs as follows: A harmonic potential has vibrational energy levels given by $E = (\nu + 1/2)\hbar\omega_0$, where $\nu = 0,1,2,\ldots$, etc. Then, allowed transitions between any two consecutive levels ($\Delta\nu = \pm 1$) in a molecule have the same energy $\hbar\omega_0$. In a more realistic anharmonic potential the level spacing shrinks with increasing $\nu$. Therefore, the transition $0 \rightarrow 1$ is at a slightly higher energy than $1 \rightarrow 2$. At room temperature, only the $\nu = 0$ state is populated appreciably.[18] This means that an approaching

photon from the laser $\hbar\omega_L$ will find the molecule most of the time in the the $\nu=0$, state and produce a Stokes-Raman process from $\nu=0$ to $\nu=1$, thus emitting a scattered photon $\omega_S$ at $\hbar\omega_S=(\hbar\omega_L-\hbar\omega_0)$. If the laser populates the $\nu=1$ state appreciably, as it would be the case under strong SERS enhancement, an incoming photon increases the chances of finding the molecule now in the $\nu=1$ state. Accordingly, if pumping to the first vibrational level is very strong, we have now the possibility of producing a Stokes-Raman process from $\nu=1$ to $\nu=2$. But the transition $1\rightarrow2$ is at a slightly smaller energy $\hbar\omega_0-\delta$. In this manner, a *shoulder* is added to the main Stokes peak and a small ''redshift'' towards the low energy side of the main line should develop. This contribution should be small, because the $0\rightarrow1$ transition is the dominant; but the mode should show as a small softening (redshift) of the peak on the Stokes side. This can be revealed in principle by a difference spectrum, as shown by Kneipp, Wang, and Kneipp,[17] their results have produced much controversy and have not yet been universally accepted.

On the anti-Stokes side, we expect the scattering process $1\rightarrow0$ at $\hbar\omega_0$ to be the dominant process. Even when the $\nu=2$ is being populated in the double pumping process $0\rightarrow1\rightarrow2$ described above, the equilibrium population of the $\nu=2$ is bound to be negligible with respect to the $\nu=1$ and, therefore, the normal $1\rightarrow0$ dominates. The intensity of the anti-Stokes signal will increase above the Boltzmann value because of the pumping (the population of $\nu=1$ is larger than the thermal one), but the frequency will not shift, because of the negligible contribution of the $\nu=2$ level in the reversed scattering process.

Vibrational pumping leads ultimately to a population imbalance of vibrations and, ultimately, to laser heating due to the inevitable relaxation of part of the energy into other modes through anharmonic interactions. There are three main possible mechanisms for single molecule laser heating: (i) off-resonance (with respect to the absorption in the molecule) Raman vibrational pumping, as described above, (ii) direct photon absorption followed by fluorescence emission and internal conversion of energy to vibrational degrees of freedom (fluorescence Stokes shift), and (iii) heating from the environment. If direct photon absorption is present it completely dominates with respect to Raman pumping, on account of the relative difference between direct absorption and third-order Raman processes. Both mechanisms are fast and for RH6G they represent the difference between excitation in the red (HeNe) or the green (514 nm, $Ar^+$-ion laser). Raman processes are instantaneous and the lifetime of exited states in dyes is sub- nano-second. In the time scale of the CCD readout (0.1–1 sec) these processes have enough time to occur and achieve thermalization if they produce heating.

A main source of information on the possibility of vibrational pumping has been the use of aS/S ratios. At a single molecule level, however, we showed already that relative fluctuations in the peaks can produce completely artificial results. Figure 5 shows an example for the 633 nm laser. The situation here is that direct absorption from the laser is small or negligible because the laser is well below the absorption maximum of RH6G which is in the green. Accordingly, the only possibility for a change in the aS/S ratio is direct Raman pumping. In this way, one expects that the larger the Raman signal on the Stokes side, the larger the pumping, and the larger the aS signal should be (above the thermal population); i.e., the larger the aS/S ratio. This is *not*, however, what it is observed in many transient spectra, as shown in Fig. 5. There are many situations in which a large (small) signal on the Stokes side is actually accompanied by a small (large) aS/S ratio; the ratio is mainly determined by fluctuations in the electromagnetic coupling to the plasmon resonances of the same type as those in Fig. 4.

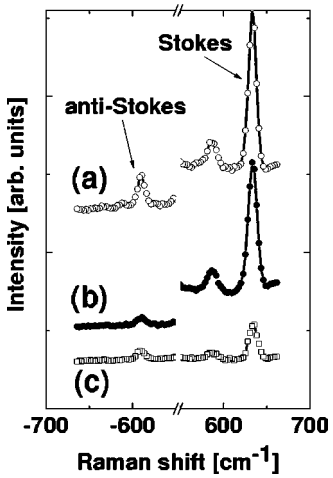


FIG. 5. Three examples of transient anti-Stokes/Stokes signals (recorded simultaneously). For the HeNe laser, the only possible mechanism changing the aS/S ratio is strong Raman pumping, for the laser is far from the maximum of the absorption peak. Larger signals should correlate with larger aS/S ratios. This is not, however, observed all the time. In these three examples (c) is actually the one with the largest aS/S ratio, while (a) is the one with the smallest. These single-molecule data show that aS/S ratios are a very unreliable measure of temperature and the intensities are mostly dominated by the hidden surface resonances of the two peaks with the environment.

Hence, since we cannot trust the aS/S ratio as a measure of pumping in a single molecule at a fixed input laser power we have to resort to other methods. The following section is devoted to alternatives to the use of anti-Stokes/Stokes ratios.

### D. Single peak fluctuations

The Boltzmann factor does not affect the anti-Stokes/Stokes ratio only. It also affects the frequency shifts (softening) and broadening of the peaks. Pumping has a similar effect, but it can be, in principle, distinguished from heating from the fact that the latter affects smaller frequencies more than higher ones, while the former can be selective and more evident for modes with larger Raman cross sections. We analyzed carefully the Stokes side of single-molecule spectra for any evidence of vibrational pumping/heating. The experimental evidence is such that it cannot be fully accounted for with a heating scenario. We shall show that there is some evidence for vibrational pumping but the effect can only be revealed not by a simple difference spectrum as in Ref. 17, but by a much more involved analysis of cross correlations of parameters. Observing the properties of a single peak

avoids automatically the problem of comparing scattering events at two different frequencies, which might be suspect to fluctuations produced by the different resonance conditions of the incoming and outgoing photons. In the frequency shift and broadening of a single peak there is hidden information on the population of different vibrational levels for that mode. It is the purpose of this section to analyze that evidence.

The Stokes peak fluctuates continuously as a function of time by small amounts, as can be readily seen in real time while the experiment is being done. Part of these fluctuations are a manifestation of molecules in slightly different situations, i.e., we are resolving the inhomogeneous broadening of the peak by measuring one molecule at a time. A relatively simple argument based on the interaction energy of the molecule with the metal surface ($\sim k_B T$), obtained from concentration isotherms, as compared to typical electronic energies ($\sim 3-4$ eV) and the effect of this on the vibrations gives an expected random change width a maximum amplitude of $\sim 0.5\ \mathrm{cm}^{-1}$. In addition to the random fluctuations of a single peak, one can expect a correlation between intensity and a redshift of the frequency and, simultaneously, a broadening of the peak. The underlying logic of this is that high intensity events are the most likely to affect the population of the different levels in a specific vibration through either pumping, or heating, or both, and this will reveal itself in a small softening of the mode and an increase in the width. Whether the effect is due to pumping or heating can only be decided by comparing two modes at different frequencies in identical experimental conditions. Heating should have a larger effect for low frequency modes to be consistent with a Boltzmann distribution.

Figure 6 shows the data for 2500 transient Raman events for the $1510\ \mathrm{cm}^{-1}$ mode. Measurements were done with the maximum power available for the HeNe laser ($\sim 6$ mW at the focal point) with the immersion $\times 100$ objective in a sample with 10 nM RH6G prepared under the conditions stated in the experimental section. The data are taken on the Stokes and anti-Stokes sides separately with a 2400 lines/mm grating to increase the resolution of the peak to $\sim 0.1\ \mathrm{cm}^{-1}$ and improve the determination of the frequency. The background is subtracted and a Lorentzian shape fitted for each spectrum. We gain from here the intensity, frequency, and width of isolated single-molecule events. We then plot in Fig. 6 the intensity of each peak as a function of its frequency for both Stokes and anti-Stokes sides. We obtain, in this manner, a correlation plot between intensity and frequency. If the two properties are completely uncorrelated, the plots should look like a uniform distribution of points, representing the contribution of the inhomogeneous broadening only.

Figure 6(a) shows that the clouds of points for the Stokes and anti-Stokes events of the $1510\ \mathrm{cm}^{-1}$ are skewed. We are seeing two effects at the same time; the inhomogeneous broadening plus the direct effect of the laser. This reveals that, in the statistical sense, larger intensity events are correlated with a softening of the peak. The fact that *both* Stokes and anti-Stokes scattering show the same correlation suggests that the reason for this effect is heating rather than

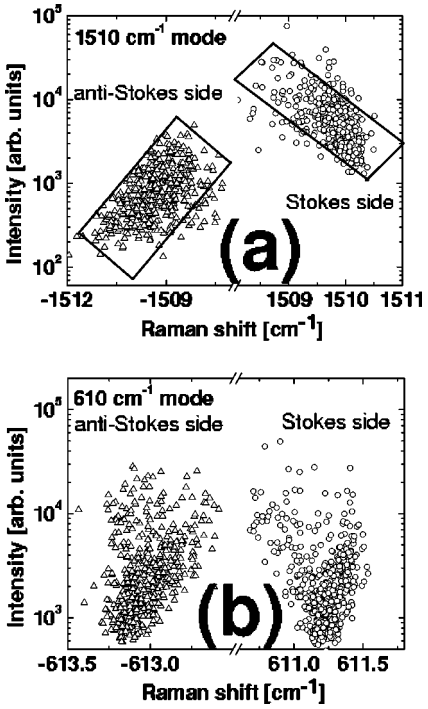


FIG. 6. Frequency-intensity correlations for (a) $1510\ \mathrm{cm}^{-1}$ and (b) $610\ \mathrm{cm}^{-1}$ modes for 2500 SERS events. Note that the intensity scales are logarithmic. In (a) the visible skewing of the data implies a correlation between high intensity and downward shifts in frequency. The dispersion of points for each case is a manifestation of molecules in slightly different situations; i.e., inhomogeneous broadening. In (b) there is a much smaller correlation between intensity and frequency shift than in (a). An estimate of the temperature needed to produce the effect in (a) is completely inconsistent with the behavior of the mode in (b). Further evidence of the difference in behavior between the two can be seen in Fig. 7.

pumping. In the case of pumping, if the $\nu=2$ level is not strongly populated as explained before, we expect the Stokes side only to soften. This is however not entirely consistent with what it is observed for a lower energy mode. Figure 6(b) shows the case of the $610\ \mathrm{cm}^{-1}$ mode again for Stokes and anti-Stokes sides. A very weak correlation between intensity and frequency can be seen, but not on the scale expected from the data in Fig. 6(a).

A few estimates are useful at this stage. Suppose that the shift observed in the $1510\ \mathrm{cm}^{-1}$ mode in Fig. 6(a) is produced by a 5% contribution of the $\nu=1\rightarrow\nu=2$ transition. This is a very conservative estimate, it is normally very hard to observe a contribution of a 5% peak (which is only slightly shifted in frequency) to the total width and frequency of the main peak. If that were the case, we would need a temperature of $T\sim 725$ K. For that temperature, the $610\ \mathrm{cm}^{-1}$ mode would have a population for $\nu=1$ of 30%, and 10% and 2.5% for $\nu=2$, and $\nu=3$, respectively. Accordingly, we would expect the $610\ \mathrm{cm}^{-1}$ to show substantial and more evident correlations between intensity and frequency than the $1510\ \mathrm{cm}^{-1}$ mode, even with a very conservative estimate of the temperature rise. This is not what it is observed, however. Further evidence that the two modes do behave differently under the same conditions in terms of their correlations among parameters comes from plots of frequency vs broadening, as shown in Fig. 7. Even without any

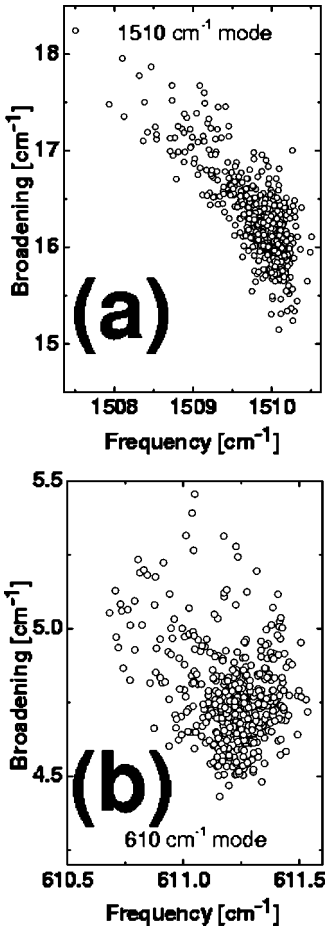


FIG. 7. Frequency-broadening correlation plots for the same modes in Fig. 6 under the same experimental conditions. A much higher degree of correlation can be seen in (a), showing a marked difference with the data in (b). A simple heating effect cannot explain the data. See the text for further details.

sophisticated correlation analysis it is possible to conclude that the 1510 $cm^{-1}$ mode has a much stronger correlation for single-molecule events between broadening and frequency, as can be seen in the comparison between Figs. 7(a) and 7(b).

Therefore, it seems that pumping is the best candidate to explain the difference between the behavior of the two modes. The reason why the 1510 $cm^{-1}$ mode is more correlated is then because it has a larger Raman cross section and its vibrational levels above $\nu=0$ are being pumped harder. But this still leaves open the question of why the anti-Stokes side of the 1510 $cm^{-1}$ mode is softened. The only possible explanation in the pumping scenario is that the $\nu=2$ vibrational state is also considerably populated, a situation that can be achieved under strong pumping conditions.

The results provided in this section demonstrate how difficult it is to prove the existence of heating or pumping effects. However, we believe that the experiments presented in this section, and the data analysis based on cross correlations of single-peak parameters, are possibly the best evidence presented so far for the possible existence of SERS pumping. The use of single peak parameters avoids the spurious artifacts normally obtained in aS/S ratios due to the presence of underlying plasmon resonances. We believe any future conclusions on the population of different vibrational levels under SERS conditions should be obtained from single-peak parameters as demonstrated here.

Finally, results with 20 mW of the 514 nm green laser line, in addition, show again only a marginal evidence for heating. With 20 mW and the $\times 100$ objective the power density at the focal point is $\sim 10^{11}$ $W/m^2$ and there is a further contribution from the local plasmon enhancement. It is remarkable that evidence for heating is only marginal in these experiments, even under direct absorption conditions; this points out the importance of rapid nonradiative recombination channels to the metal which both: (i) remove energy from the molecule before it can be thermalized by anharmonic processes and transformed into an effective temperature, and (ii) quench the fluorescence.

In order to provide a qualitative theoretical understanding of the results in this paper and make several connections among results we study a schematic model of colloid cluster in the following section.

## IV. THEORY

The optical properties of nanometer-sized metallic objects are normally complex and one must resort to approximations which are case dependent. This holds even for periodic structures which are substantially more complex than the dielectric counterparts due to the frequency dependence of the dielectric function.[19] We work with the discrete-dipole approximation (DDA) method of Purcell and Pennypacker.[20–22] A minimum of details are given here and the reader is referred to the original literature[20–22] for further details.

A given geometry is divided into small cells with characteristic dimension $d$ ($d \ll \lambda$; $\lambda$ = wavelength of the light). The polarization vector at the $i$th cell $\vec{P}_i$ is

$$\vec{P}_i = \alpha_i \ \vec{E}^i_{\text{tot}}, \tag{1}$$

where $\alpha_i$ is the local scalar polarizability and $\vec{E}_{\text{tot}}$ the total electric field at site $i$, given by

$$\vec{E}^i_{\text{tot}} = \vec{E}^i_{\text{dip}} + \vec{E}^i_0, \tag{2}$$

where $\vec{E}^i_{\text{dip}}$ is the field produced by all other dipoles with $j \neq i$ and $\vec{E}^i_0$ is the field produced by an incident laser field (in the planewave approximation) with wave vector $k = 2\pi/\lambda$ and frequency $\omega$. The electric field at cell $i$ produced by all the other cells is[22–24]

$$\vec{E}^i_{\text{dip}} = -\sum_{j \neq i} \hat{A}_{ij} \cdot \vec{P}_j, \tag{3}$$

where

$$\hat{A}_{ij} \cdot \vec{P}_j = \frac{e^{ikr_{ij}}}{r^3_{ij}} \left\{ k^2 \vec{r}_{ij} \times (\vec{r}_{ij} \times \vec{P}_j) + \frac{(1 - ikr_{ij})}{r^2_{ij}} \times [r^2_{ij} \vec{P}_j - 3\vec{r}_{ij}(\vec{r}_{ij} \cdot \vec{P}_j)] \right\}, \tag{4}$$

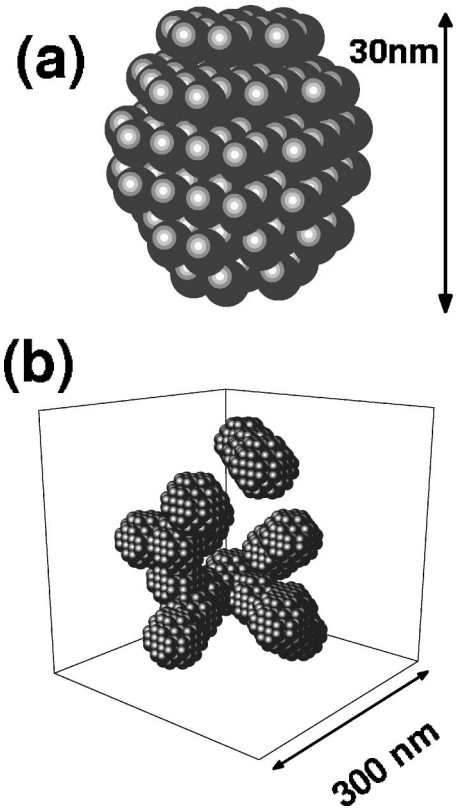


FIG. 8. (a) A single colloid of 30 nm in diameter is modeled with 136 single-polarizable cells as in the original paper by Purcell and Pennypacker (Ref. 20). (b) A snapshot into a configuration of 20 colloids within a volume of 300 $nm^3$. The configuration is set up by choosing random positions inside the volume while avoiding direct overlaps among the colloids. The incident EM wave travels along the vertical direction $\hat{z}$.

and where $r_{ij}=|\vec{r}_{ij}|$ $(i\neq j)$ is the distance between cells $i$ and $j$, respectively. The solution of the $3N\times 3N$ linear inhomogeneous equations

$$\alpha_i^{-1}\vec{P}_i+\sum_{j\neq i}\hat{A}_{ij}\cdot\vec{P}_j=\vec{E}_0^i \tag{5}$$

gives the answer to the problem. All the fields have a $e^{-i\omega t}$ time dependence.

We aim at understanding qualitative aspects of the problem in this section; several approximations going from the size of the colloids to the shape of the clusters, to the number of cells used in each individual colloid will be necessary. We are not aiming at reproducing exactly the experimental conditions which have many unknown parameters. The exact nature of the geometry of the clusters formed by colloid coming in close proximity is, for example, not known. Many trends can be understood, however, in simplified models and we shall make *ad hoc* approximation where necessary.

In Fig. 8(a) we show the basic DDA decomposition of a single colloid in polarizable cells. A single colloid of 30 nm in diameter is modelled with 136 single-polarizable cells as in the original paper by Purcell and Pennypacker.[20] This decomposition has been shown to reproduce very accurately most of the basic single-particle scattering properties (Mie), as well as the near field down to very small distances close to the surface of the colloids. Figure 8(b) shows a cluster of 20 colloids in a volume of 300 $nm^3$; we use this cluster as a representative situation inside the colloidal fluid when the KCl has partly nucleated the particles and brought them into close proximity. We used slightly smaller colloids than the ones used in the experiment to avoid using too many cells or cells which are too big for the approximations in the DDA to be valid.

An incident plane wave comes along from the vertical direction on the cluster shown in Fig. 8(b) and the self-consistent polarizations in the cells are calculated by means of an iterative *conjugate gradient algorithm* as developed by Markel.[25] Intensity maps inside the cluster can be done only along specific planes; they all show the same qualitative features. Figure 9 shows an example of an intensity map along one of the many possible vertical planes cutting the cluster through the middle. We perform calculations at three different wavelengths corresponding to the laser (633 nm) and at the Stokes and anti-Stokes frequencies, assuming a Stokes shift of 1000 $cm^{-1}$ (typical for organic molecules).

The main purpose of this calculation is to present a physical basis for the anti-Stokes/Stokes fluctuations. A careful inspection of the intensity patterns reveals that a single point can be strongly coupled to the laser frequency while showing very different amounts of coupling to the Stokes and anti-Stokes energies. A molecule sitting in that place in the solution will have a natural asymmetry in the intensity of the two peaks, which is *purely electromagnetic* and it is not related to temperature.

The main qualitative lesson we can learn from the simulations is that asymmetries in anti-Stokes/Stokes signals are a natural consequence of having the molecule in a medium with resonant plasmon interactions. This will naturally affect single molecular spectra and the interpretation of aS/S ratios, as demonstrated in the previous sections.

Moreover, further analysis of the intensity patterns in these maps reveals several hints of features seen in actual experiments. In Figure 10 we plot for the maps shown in Fig. 9 the aS/S ratio at each point vs the laser intensity in the same place. Since the incident wave is normalized to an intensity$=1$, the laser intensity map is automatically an *enhancement factor map*. So Fig. 10 shows the aS/S ratio as a function of the local enhancement factor for $200\times 200=4\times 10^4$ points in the maps of Fig. 9. Similar results are obtained for maps along other planes. The data in Fig. 10 show a striking overall correlation between enhancement factor and larger aS/S ratios. The important details of the data are that (i) the average of all these points is larger than 1 ($\sim 1.3$), implying that in situations of high concentration of molecules one would obtain an overall aS/S ratio above the Boltzmann factor prediction (as it is almost always the case with the 633 nm laser), and (ii) when looking at individual events, however, as it would be the case in SMD, it is possible to have isolated cases in which the signal is low (small enhancement) but the aS/S ratio is high (point $A$ in the figure), or cases where the signal is large but the aS/S ratio is suppressed (point $B$). Accordingly, a simple calculation like this then can explain qualitatively many aspects of single-molecule data like that in Fig. 5.

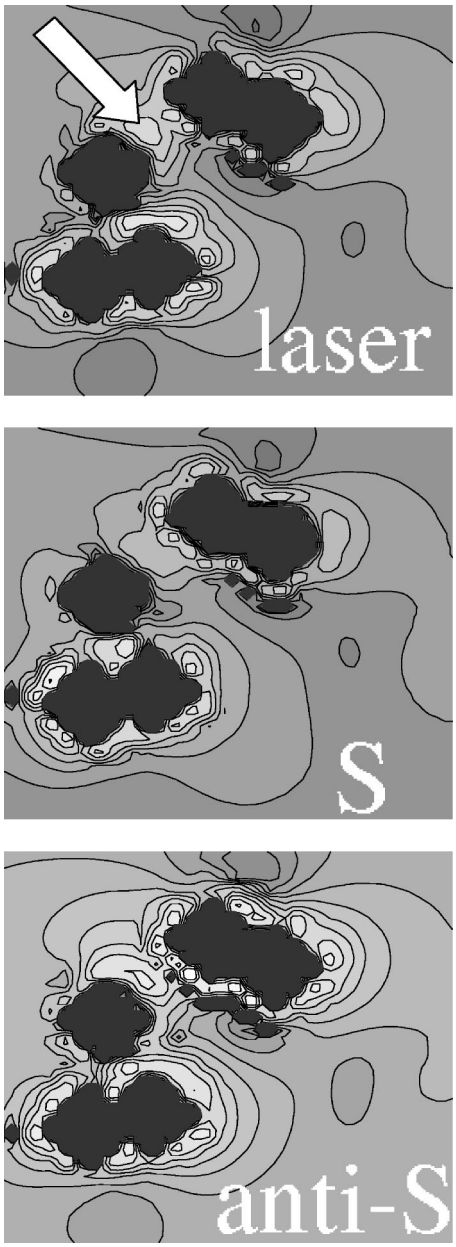


FIG. 9. Three intensity maps (enhancement factors) at the laser (top), Stokes (middle), and anti-Stokes (bottom) frequencies. The intensities are on a logarithmic scale of colors from 0.01 (black) to 250 (white). The maps are along the plane of incidence of the incoming wave cutting the cluster through the middle. The interior of the colloids which are cut through appear as dark black features in the map. The arrow on the map at the top exemplifies a position where the laser intensity is relatively high, but the Stokes and anti-Stokes fields are coupled to different extents in the same place (see the equivalent place in the middle and bottom maps). A molecule sitting in that position will have an asymmetry between the aS and S signals, which is purely electromagnetic and has no relation to temperature changes. The phenomenon is widespread over the intensity map and supports the idea that aS/S asymmetries are purely electromagnetic in origin.

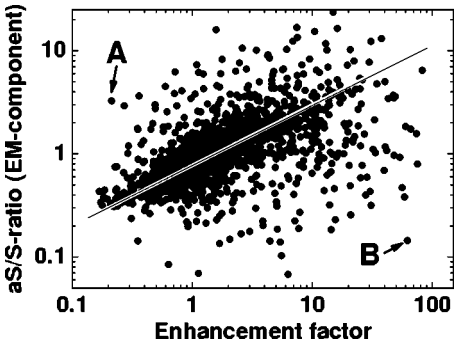


FIG. 10. aS/S ratio as a function of normalized laser intensity (or enhancement factor) for $4\times10^5$ points in the maps shown in Fig. 9. An overall correlation between the aS/S ratio and the enhancement factor can be observed. Note the presence of a double log-scale. Since the intensity of the largest signals dominates the spectra in the presence of many molecules, and they tend to have aS/S ratios $>1$, this results ultimately in overall aS/S ratios larger than unity for the 633 nm laser. This is observed all the time for the HeNe excitation. When looked individually (as done in SMD experiments) it is possible to have weak signals with high aS/S ratio (as exemplified with point *A* in the graph) or large signals with small aS/S ratio (B), as seen often in experiments (see Fig. 5).

## V. CONCLUSIONS

We have studied several aspects of SMD in SERS related to the evidence of hidden plasmon resonances as well as laser heating and/or vibrational pumping. We find compeling evidence that hidden plasmon resonances are the most important factor altering the relative intensity of different peaks. We also established that anti-Stokes/Stokes ratios can only be used if there is an underlying understanding of the electromagnetic contribution to the peaks on both sides of the laser and, in addition, that they are generally not very good indicators of temperatures and/or pumping. A few hints of heating/vibrational pumping in SMD can only be obtained in a statistical sense once detailed correlations between the parameters of the Stokes scattering are analyzed. A mode with a higher Raman cross section, such as 1510 $cm^{-1}$, displays a very different behavior from lower energy modes like the 610 $cm^{-1}$ in a way, which is not entirely consistent with a temperature rise and suggest some degree of pumping. A marginal skewing of the intensity-frequency plots for the 610 $cm^{-1}$ mode and a mild correlation between frequency and broadening suggests that there might be a small contribution from heating in the total effect. This is acceptable if we take into account that pumping will result inevitably in a small conversion of energy to other modes through anharmonic interactions and, therefore, a small amount of heating. The most likely situation suggested by our data is that both effects play a role to different extents.

Our work here leaves completely aside the issue of the power dependence of the SERS signals. In this paper we have established the techniques and methods to be used (cross correlations among parameters of the same peak) to reveal trends in transient single-molecule vibrational pumping/heating. Our results reveal that there might be a contribution from pumping and heating to single-molecule spectra, but both seem to be small in comparison with other claims.[17,26] A companion separate study with cross correlations among parameters at different incident powers is in progress and will be published elsewhere.[27]

## ACKNOWLEDGMENTS

P.G.E. and L.F.C. acknowledge partial support for this work by the Engineering and Physical Sciences Research Council (EPSRC) of the U.K. under Grants No. GR/R28775 and GR/T06124. R.C.M. acknowledges partial support from

the National Physical Laboratory (NPL) in the U.K., and the hospitality of the McDiarmid Institute for Advanced Materials and Nanotechnology, Victoria University of Wellington, New Zealand where part of the experiments were performed. The authors are indebted to Dr. Richard Tilley at Victoria University of Wellington for help with the analysis of their colloids.

[1] M. Moskovits, Rev. Mod. Phys. **57**, 783 (1985).
[2] A. Otto, in *Light Scattering in Solids*, edited by M. Cardona and G. Güntherodt (Springer, Berlin, 1984), p. 289.
[3] K. Kneipp, H. Kneipp, I. Itzkan, R. R. Dasari, and M. S. Feld, J. Phys.: Condens. Matter **14**, R597 (2002).
[4] P. Etchegoin, L. F. Cohen, H. Hartigan, R. J. C. Brown, M. J. T. Milton, and J. C. Gallop, J. Chem. Phys. **119**, 5281 (2003).
[5] R. C. Maher, L. F. Cohen, and P. Etchegoin, Chem. Phys. Lett. **352**, 378 (2002).
[6] P. Etchegoin, R. C. Maher, L. F. Cohen, H. Hartigan, R. J. C. Brown, M. J. T. Milton, and J. C. Gallop, Chem. Phys. Lett. **375**, 84 (2003).
[7] A. Otto, J. Raman Spectrosc. **33**, 593 (2002).
[8] P. C. Lee and D. Meisel, J. Phys. Chem. **86**, 3391 (1982).
[9] Dr. Richard Tilley (private communication).
[10] *American Institute of Physics Handbook*, 3rd ed. (McGraw-Hill, New York, 1972).
[11] S. Nie and S. R. Emory, Science **275**, 1102 (1997).
[12] H. Jakobi and H. Kuhn, Z. Elektrochem. Angew. Phys. Chem. **66**, 46 (1962).
[13] J. Jiang, K. Bosnick, M. Maillard, and L. Brus, J. Chem. Phys. B **107**, 9964 (2003).
[14] N. Hayazawa, Y. Inouye, Z. Sekkat, and S. Kawata, Chem. Phys. Lett. **335**, 369 (2001).
[15] W. Hayes and R. Loudon, *Scattering of Light by Crystals* (Wiley, New York, 1978), p. 115.
[16] T. L. Haslett, L. Tay, and M. Moskovits, J. Chem. Phys. **133**, 1641 (2000).
[17] K. Kneipp, Y. Wang, and H. Kneipp *et al.*, Phys. Rev. Lett. **76**, 2444 (1996).
[18] R. C. Maher, L. F. Cohen, P. Etchegoin, H. Hartigan, R. Brown, and M. Milton, J. Chem. Phys. **120**, 11746 (2004).
[19] K. Sakoda, N. Kawai, T. Ito, A. Chutinan, S. Noda, T. Mitsuyu, and K. Hirao, Phys. Rev. B **64**, 045116 (2001).
[20] E. M. Purcell and C. R. Pennypacker, Astrophys. J. **186**, 705 (1973).
[21] W. H. Yang, G. C. Schatz, and R. P. van Duyne, J. Chem. Phys. **103**, 869 (1995).
[22] J. J. Goodman, B. T. Draine, and P. J. Flatau, Opt. Lett. **16**, 1198 (1991).
[23] R. Rojas and F. Claro, J. Chem. Phys. **98**, 998 (1993).
[24] *Handbook of Optical Constants of Solids*, edited by E. D. Palik (Academic, New York, 1985).
[25] V. A. Markel, L. S. Muratov, M. I. Stockman, and T. F. George, Phys. Rev. B **43**, 8183 (1991).
[26] A. G. Brolo, A. C. Sanderson, and A. P. Smith, Phys. Rev. B **69**, 045424 (2004).
[27] R. C. Maher, P. G. Etchegoin, and L. F. Cohen (unpublished).